

Article

A Novel Integrated Electronic Lighting Driver Circuit for Supplying an LED Projection Lamp with High Power Factor and Soft Switching Characteristics

Chun-An Cheng , Ching-Min Lee , En-Chih Chang *, Sheng-Hong Hou, Long-Fu Lan and Cheng-Kuan Lin

Department of Electrical Engineering, I-Shou University, Kaohsiung City 84001, Taiwan; cacheng@isu.edu.tw (C.-A.C.); cmlee@isu.edu.tw (C.-M.L.); isu11001001m@cloud.isu.edu.tw (S.-H.H.); isu11001004m@cloud.isu.edu.tw (L.-F.L.); isu11001014m@cloud.isu.edu.tw (C.-K.L.)

* Correspondence: enchihchang@isu.edu.tw; Tel.: +886-7-6577711 (ext. 6642)

Abstract: The traditional light source of projection lamps adopts a halogen lamp, which has the advantages of high brightness, but its luminous efficiency is not good and consumes energy. A light-emitting diode (LED) has the characteristics of high luminous efficiency and energy savings and can be used as a new light source for projection lamps. The conventional two-stage electronic lighting driver circuit for supplying an LED projection lamp is composed of an AC-DC converter with power factor correction (PFC) as the first stage and a DC-DC converter for providing rated lamp voltage and current as the second stage. The conventional LED projection lamp driver circuit has more circuit components, a higher cost and limited efficiency. Therefore, this paper proposes a novel electronic lighting driver circuit for supplying an LED projection lamp with PFC function, which integrates a modified stacked dual boost converter and a half-bridge LLC resonant converter into a single-stage power-conversion circuit. The inductor inside the modified stacked boost converter is designed to operate at discontinuous conduction mode (DCM) for the driver circuit achieving PFC. Wide bandgap semiconductor devices silicon carbide (SiC)-based Schottky diodes are utilized to reduce power diode losses, and soft switching is implemented in the proposed LED projector lamp driver circuit to reduce the switching losses of the power switches and thus improve circuit efficiency. This paper has completed a single-stage prototype driver circuit for an LED projection lamp with PFC function, and the prototype circuit has a high power factor ($PF > 0.98$), low input current total-harmonic-distortion ($THD < 6\%$) and high efficiency ($> 89\%$) in the case of an AC input power supply with an RMS value of 110 volts, and both power switches have the characteristics of soft switching.

Keywords: electronic lighting; LED; projection lamp; power factor correction; soft switching; single-stage



Citation: Cheng, C.-A.; Lee, C.-M.; Chang, E.-C.; Hou, S.-H.; Lan, L.-F.; Lin, C.-K. A Novel Integrated Electronic Lighting Driver Circuit for Supplying an LED Projection Lamp with High Power Factor and Soft Switching Characteristics. *Electronics* **2023**, *12*, 4642. <https://doi.org/10.3390/electronics12224642>

Academic Editors: Diego Gonzalez Lamar and Aitor Vázquez Ardura

Received: 27 September 2023
Revised: 5 November 2023
Accepted: 10 November 2023
Published: 14 November 2023



Copyright: © 2023 by the authors. Licensee MDPI, Basel, Switzerland. This article is an open access article distributed under the terms and conditions of the Creative Commons Attribution (CC BY) license (<https://creativecommons.org/licenses/by/4.0/>).

1. Introduction

A projection lamp, often used in devices like projectors, stage lighting and some types of microscopy, serves several important functions depending on the specific application. Here are the primary functions of a projection lamp: (1) Illumination: The primary function of a projection lamp is to provide a bright and focused light source. In the context of a projector, this light source is essential for displaying images or videos on a screen or surface. The intensity and quality of the illumination directly impact the clarity and visibility of the projected content. (2) Brightness: Projection lamps are designed to produce high-intensity light, which is necessary for creating a visible image, especially in well-lit environments. The brightness of the lamp is typically measured in lumens, and a brighter lamp allows for larger and more vivid projections. (3) Color Rendering: Depending on the type of lamp used, it can influence the color accuracy and rendering of the projected image. Different lamps emit light at varying color temperatures, which can impact the overall color quality of the projection. Some lamps are designed to provide more accurate color reproduction,

which is crucial for applications like home theater projectors or professional photography. (4) Longevity: Projection lamps need to have a reasonable lifespan to be cost-effective. While the specific lifespan varies based on the lamp technology, manufacturers aim to provide lamps that can last for hundreds or even thousands of hours of use. (5) Heat Management: Projection lamps can generate a significant amount of heat during operation. Proper heat management and cooling systems are often integrated into the projector or lighting fixture to ensure the lamp operates safely and efficiently. (6) Lamp Control: Projectors and other devices equipped with projection lamps typically include control mechanisms to adjust the lamp's brightness, color temperature and other settings to suit different viewing conditions and content types. This control allows for customization and optimization of the projected output. (7) Instant On/Off: In the case of projection lamps that have an instant on and off feature, this feature comes in handy for applications that require a quick startup and shutdown. (8) Energy Efficiency: Energy efficiency is an important consideration, especially as technology advances. Some projection lamps have environmentally friendly energy-saving features that not only reduce operating costs but also reduce power consumption, which is good for the environment. In summary, the functions of a projection lamp include providing illumination, brightness, color rendering, lifetime, heat management, control, instant on/off functionality and energy efficiency. Together, these functions determine the quality and performance of a projection system in a variety of applications [1].

Conventional projection lamps, which typically include halogen and metal halide lamps, have been widely used in various projection and lighting applications for many years. The advantages of conventional projection lamps are: (A) Brightness: Conventional projection lamps are known for their high brightness levels, making them suitable for large-screen projections in well-lit environments. They can produce intense and vibrant images. (B) Color Accuracy: Some types of conventional lamps, such as metal halide, can provide good color accuracy and color rendering, making them suitable for applications where color fidelity is important, like professional photography or video production. (C) Cost: In some cases, conventional projection lamps can be more affordable upfront compared to certain newer technologies like laser projectors or high-end LED projectors. This can make them a cost-effective choice for certain applications. (D) Availability: Conventional projection lamps are widely available, making them easy to replace when needed. This availability also means that replacement lamps come in various wattages and color temperatures, providing flexibility in selecting the right lamp for a specific application [2].

On the other hand, the disadvantages of conventional projection lamps are: (A) Limited Lifespan: Traditional projection lamps have a relatively short lifespan compared to newer lighting technologies. They may need to be replaced frequently, which can increase maintenance costs over time. (B) Heat Generation: Conventional projection lamps can generate a significant amount of heat during operation. This not only requires effective cooling systems but can also make them unsuitable for some small, enclosed spaces or delicate projection materials. (C) Energy Inefficiency: Conventional lamps, such as halogen lamps, are not energy-efficient. They waste a significant amount of energy as heat, which can contribute to higher operating costs. (D) Warm-Up and Cool-Down Time: Some conventional projection lamps, like metal halide lamps, may require a significant amount of time to warm up to full brightness and cool down after use. This can be inconvenient in situations where quick on/off capabilities are needed. (E) Environmental Impact: Conventional projection lamps are less environmentally friendly due to their energy inefficiency and the fact that they contain hazardous materials like mercury (in the case of some metal halide lamps). The disposal of these lamps must follow specific regulations. (F) Bulky Size: Conventional projection lamps are often larger and bulkier than their newer counterparts, which can limit their use in compact or portable projection devices. (G) Maintenance Costs: The need for frequent lamp replacements, along with the associated labor and downtime, can result in higher maintenance costs over time [2].

To address these issues, LED projectors offer several advantages over traditional projection lamps and lighting technologies. The key advantages of LED projection lamps

are: (1) Energy Efficiency: LED projection lamps are highly energy-efficient, consuming significantly less power than traditional lighting sources. (2) Longevity: LEDs have a much longer lifespan compared to traditional lamps. LED projection lamps can last up to 25,000 h or more, reducing the frequency of lamp replacements and maintenance costs. (3) Brightness and Color Accuracy: LED projection lamps can produce bright and vibrant colors, making them ideal for applications where color accuracy is crucial, such as home theaters, professional presentations and digital signage. (4) Instant On/Off: LEDs provide instant illumination without the warm-up time required by some other lamp types. This feature is especially useful in situations where immediate lighting is needed. (5) Cool White Light: Many LED projection lamps produce a cool white light that is suitable for a wide range of applications, from outdoor lighting to task lighting. (6) Dimmability: LED projection lamps can often be dimmed to adjust the light output to the desired level, providing flexibility in lighting design and energy savings when full brightness is not required. (7) Durability: LEDs are solid-state lighting devices, which means they are more durable and resistant to shock and vibrations compared to fragile incandescent and fluorescent bulbs. (8) Reduced UV Emissions: Unlike some other light sources, LEDs emit very little ultraviolet (UV) radiation, which can be harmful to people and sensitive materials. This makes LED projection lamps safer for use in museums, art galleries and other environments where UV exposure should be minimized. (9) Environmental Benefits: LED projection lamps are environmentally friendly due to their lower energy consumption and longer lifespan. They also contain fewer hazardous materials, such as mercury, which is commonly found in fluorescent lamps. (10) Low Maintenance: The long lifespan of LED projection lamps means less frequent maintenance and replacement, reducing the overall cost of ownership. (11) Compatibility: LED projection lamps are available in various shapes and sizes, making them suitable for retrofitting existing fixtures and a wide range of applications, including residential, commercial and industrial settings. (12) Directional Light Output: LEDs emit light in a specific direction, which can be advantageous in applications where the precise control of light direction and distribution is needed, such as spotlights and projectors [3,4].

Overall, LED projection lamps offer a combination of energy efficiency, a long lifespan, durability, color accuracy and versatility, which makes them a popular choice for a wide range of lighting applications. Some suitable application areas for LED projection lamps include: (1) Outdoor Events: LED projection lamps can be used for outdoor movie nights, sports screenings and other events where a large, bright display is required. (2) Business and Education: LED projection lamps are used in classrooms and conference rooms for presentations, lectures and interactive learning. They offer bright and clear visuals, making them ideal for educational and professional settings. (3) Art Installations: Artists often use projection lamps for large-scale art installations, allowing them to project images, videos or dynamic visuals onto buildings, walls or other surfaces. (4) Advertising and Marketing: LED projection lamps are used for creative advertising campaigns, projecting brand messages or promotional content onto buildings, sidewalks or other public spaces. (5) Entertainment and Events: LED projection lamps are commonly used in concerts, festivals and events for projecting visuals onto stages, screens and backdrops to enhance the overall entertainment experience. (6) Architectural Lighting: projection lamps can be used to illuminate the facades of buildings, bridges and monuments, creating stunning architectural lighting effects [5–14].

As shown in Figure 1, the conventional AC-DC driver circuit that powers the LED projector lamp is a two-stage power converter consisting of an AC-DC converter with power factor correction (PFC) and a DC-DC converter that provides the rated voltage and current. In addition, an AC-DC converter controller is required to control the front-stage circuit and a DC-DC converter controller is used to control the rear-stage circuit. The half-bridge LLC resonant converter, a widely used power converter suitable for use as a post-stage DC-DC power converter in conventional AC-DC driver circuits powering LED projector lamps, is favored in some cases because of its various advantages: (1) High

Efficiency: The half-bridge LLC resonant converter operates with high efficiency, especially for high power applications. It reduces switching losses and minimizes power dissipation, which improves overall efficiency. (2) Soft switching: The half-bridge LLC resonant circuit topology enables soft switching of the power switches, which reduces electromagnetic interference (EMI) and minimizes stress on components, extending their life. (3) Wide Operating Range: Half-bridge LLC resonant converters can operate over a wide range of input voltages and output loads, making them versatile and suitable for a wide variety of applications. (4) EMI Reduction: The soft switching characteristics and resonant behavior of half-bridge LLC converters help reduce EMI, which is important in applications where EMI control is required. (5) High Power Density: High efficiency and low component stress allow for higher power density designs, which means smaller and lighter power supplies or inverters. (6) Good Transient Response: Half-bridge LLC resonant converters have good transient response characteristics, which means they can respond quickly to load changes while maintaining a stable output voltage. (7) Reduced Heat: Lower switching losses reduce heat generation, resulting in a smaller, more cost-effective cooling solution. (8) Reduced Component Stress: The resonant operation of half-bridge LLC converters reduces stress on components such as capacitors and inductors, resulting in a longer component life and improved reliability. (9) Compatible with a wide range of applications: Half-bridge LLC converters are suitable for a wide range of applications including renewable energy systems, electric vehicle chargers, server power supplies and more. (10) Power Factor Correction (PFC): Half-bridge LLC resonant converters provide power factor correction, helping to ensure that the power factor of the load and input source are close to unity [15–19].

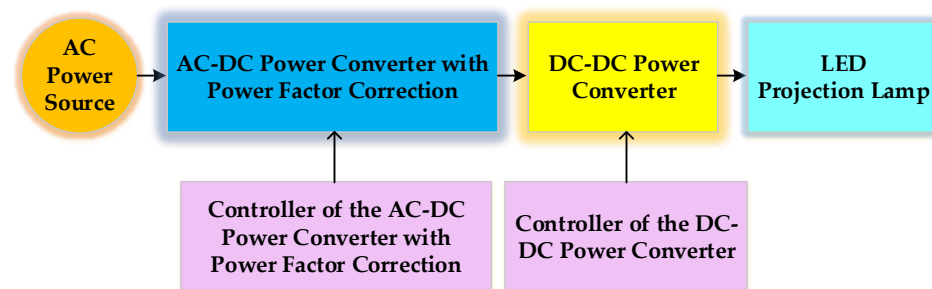


Figure 1. Block diagram of the conventional two-stage electronic lighting driver circuit for supplying an LED projection lamp with a power-factor-correction characteristic.

Refs. [15,16] describe a two-stage electronic lighting driver circuit suitable for powering LED projector lamps, which consists of a boost converter with a high power factor as the first-stage circuit, a half-bridge LLC resonant converter as the second-stage circuit and power switches and output power diodes with soft switching characteristics. Reference [17] presents a two-stage electronic lighting driver circuit suitable for powering an LED projector lamp, where the first stage is a boost converter with high power factor characteristics and the second stage is a half-bridge CLCL resonant converter. Under full load operation, the power switches on the primary side turn on in ZVS mode and turn off in a very low current state, which is named as “quasi-ZCS mode”. In addition, the ZVS turn-on characteristic of the power switch and the ZCS turn-off characteristic of the power diode are realized at full load. Reference [18] describes a two-stage electronic lighting driver circuit suitable for powering LED projector lamps, where the first stage is a boost converter with power factor correction and the second stage is a dual buck converter operating in a quasi-resonant zero-voltage switching state in order to reduce the switching losses of the power switches and thus significantly improve the circuit efficiency. Reference [19] describes a two-stage LED driver circuit where the first stage is a boost converter with input current shaping and the second stage is an asymmetric half-bridge converter with soft switching for street lighting applications, and this version is also suitable for powering LED projection lights. Furthermore, the transformer design (with asymmetric secondary winding) in the converter presented in [19] has the advantage of minimizing conduction losses, while the dead-time

converter model optimizes its duration and reduces the switching losses of the MOSFETs and diodes.

The literature [20–23] has developed a number of single-stage LED driver circuits that integrate an AC-DC power converter and a DC-DC power converter suitable for powering projection lamps. In order to reduce the number of power switches and circuit components and to improve the overall circuit efficiency of the conventional two-stage version, a novel AC-DC integrated electronic lighting driver circuit that integrates a modified stacked boost converter with a half-bridge LLC resonant converter for supplying an LED projection lamp with PFC and soft switching capabilities is proposed in [24]. This paper is an extended and improved version of [24]. An existing driver circuit with input current shaping (ICS) and soft switching features, which consists of a front AC-DC full-wave bridge rectifier and a rear DC-AC circuit combining a stacked dual boost converter and a half-bridge resonant inverter for driving a piezoelectric ceramic actuator, has been presented in [25]. The modified stacked dual boost converter developed in this paper is capable of economizing two diodes and one capacitor in comparison to the traditional stacked dual boost one shown in [25]. By designing the series inductance of the modified stacked boost converter to operate in the discontinuous-conduction-mode (DCM), the electronic lighting driver circuit has a PFC function. The recently novel wide bandgap semiconductor device silicon carbide (SiC) is a compound semiconductor material composed of silicon (Si) and carbon (C). The new semiconductor material SiC has a strong bonding force and is characterized by the following features: (1) Thermal stability: The liquid layer of SiC does not exist at an atmospheric pressure and sublimates only at temperatures higher than 2000 °C. (2) Mechanical stability properties: SiC has a Mohs hardness of 9.3, which is comparable to diamond, with a Mohs hardness of 10. (3) Chemical stability: SiC is inert to almost all acids and alkalis. Since the dielectric breakdown field strength of silicon carbide is about 10 times that of silicon, it can withstand voltages as high as 600 V to several thousand V. In addition, the impurity concentration can be adjusted to be higher than that of silicon devices, and the thick drift layer (drift diffusion) can be made thinner. The impedance component of a high-voltage power device is almost always the impedance of the drift layer, and the impedance value is proportional to the thickness of the drift layer. Since silicon carbide can make the drift layer thinner, it is possible to produce high-voltage components with very low on-resistance per unit area. Theoretically, if the withstand voltage is the same, the impedance of the drift layer per unit area can be reduced to 1/300 of that of silicon. In order to solve the problem of the on-resistance increasing with the withstand voltage, in the past, the silicon power devices mainly used minority carrier devices (bipolar devices). However, there are heating problems due to high switching losses and limitations in high-frequency driving. Most high-speed carrier devices (carrier devices), such as Schottky diodes or MOSFETs, are made of SiC novel material instead of the conventional Si material, which is characterized by a high withstand voltage, low on-resistance and high speed. In addition, since the bandgap of SiC is about three times wider than that of Si, it can operate at higher temperatures than Si [26]. SiC's high-speed component structure using a Schottky barrier diode (SiC-SBD) structure realizes a high withstand voltage diode of 600 V or more compared to Si using an SBD (Si-SBD) of about 200 V. As a result, the recovery loss can be significantly reduced by replacing the current mainstream high-speed PN junction diode (silicon-fast recovery diode (Si-FRD)). The initial voltage of SiC-SBD is the same as that of Si-FRD, but the temperature dependence is different from that of Si-FRD. The higher the temperature of SiC-SBD, the higher the operating resistance and the higher the voltage drop V_f during the forward conduction. Since SiC-SBDs are less prone to thermal runaway, they are ideal for parallel use. When an SiC-SBD switches from forward to reverse, it passes a large amount of transient current. During this time, it is in reverse bias, which can cause significant losses. This is due to the fact that the small number of carriers that accumulate in the drift layer when current is applied in the forward direction contribute to the conductivity during the period before they are eliminated (buildup time). The higher the forward current or the higher the temperature,

the longer the recovery time and the higher the recovery current, resulting in significant losses. On the other hand, since SiC-SBD is a majority carrier element (field effect transistor) and does not use minority carriers for electrical conduction, the accumulation of minority carriers theoretically does not occur. By simply generating a small current to discharge the capacitance on the bonding surface, the loss can be greatly reduced compared to that of Si-FRD. Since this transient current is virtually independent of the temperature and forward current, it enables stable, high-speed recovery regardless of the environment. In addition, it reduces the noise generated by the recovery current. Typically, wide-bandgap semiconductor silicon carbide devices with Schottky barrier diodes lose only 1% of silicon energy during the reverse recovery phase. With virtually no tail current, turn-off is faster, and losses are greatly reduced. Because less energy is dissipated, silicon carbide devices can switch at higher frequencies and improve efficiency. Therefore, silicon carbide is considered a promising material for power components that can surpass the limits of silicon [27]. In addition, the wide bandgap semiconductor devices SiC-based Schottky diodes are utilized to lower power diode losses, and the resonant tank circuit of the half bridge LLC resonant converter sub-circuit is appropriately designed; thus, two power switches can realize zero-voltage-switching (ZVS) and two output diodes can realize zero-current-switching (ZCS) characteristics in the proposed electronic lighting driver circuit in order to increase the circuit efficiency. This paper is organized as follows. Section 2 describes and analyzes the operating modes of the integrated electronic lighting driver circuit that powers the LED projection lamp and provides design guidelines for some circuit parameters. In Section 3, experimental results of a prototype electronic lighting driver circuit for supplying an LED projection lamp are demonstrated. Finally, Section 4 gives some conclusions.

2. Descriptions and Analysis of Operational Modes in the Proposed AC-DC Integrated Electronic Lighting Driver Circuit for Supplying an LED Projection Lamp

Figure 2 shows the proposed AC-DC integrated electronic lighting driver circuit for powering an LED projection lamp that incorporates a modified stacked dual boost converter with power factor correction and a half-bridge LLC resonant converter. The modified stacked dual boost converter with a power factor correction sub-circuit includes two diodes (D_1 and D_2) and the stacked dual boost circuits. In addition, the capacitor C_{in1} , the diode D_3 , the switch S_1 , the inductor L_B , the intrinsic diodes of S_2 and the DC-linked capacitor C_{bus} form one of the dual boost circuits, whereas the capacitor C_{in2} , the diode D_4 , the switch S_2 , the inductor L_B , the intrinsic diodes of S_1 and the DC-linked capacitor C_{bus} form the other dual boost circuit. The dual boost circuits are stacked in an up-down manner, hence the name “stacked dual boost converter”, and share the inductor L_B as well as the DC-linked capacitor C_{bus} . Since the sum of the input powers of the stacked dual boost converter is equal to the total power for providing with the LED projection lamp, the current stress on the power switch can be halved by using a stacked power conversion circuit topology. The half-bridge LLC resonant converter sub-circuit consists of a DC-linked capacitor C_{bus} , two switches (S_1 and S_2), a resonant inductor (L_r), a resonant capacitor (C_r), a center-tapped transformer T (where n_p and n_s are the turns of the primary side and secondary side, respectively), with a magnetic inductor L_m , two diodes (D_5 and D_6) and a capacitor (C_o), and the LED projection lamp. The modified stacked boost converter with a power factor correction sub-circuit and the half-bridge LLC resonant converter sub-circuit share two power switches (S_1 and S_2) and a DC-linked capacitor C_{bus} . In addition, by operating the inductor L_B in discontinuous conductive mode (DCM), input current shaping can be achieved naturally by using commonly used control integrated circuits (ICs), eliminating the need for more expensive PFC control ICs.

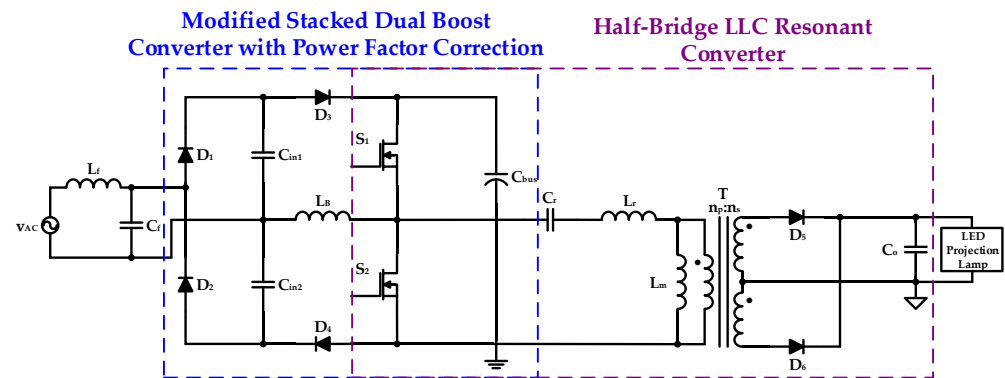


Figure 2. The proposed AC-DC integrated electronic lighting driver circuit for supplying an LED projection lamp with a power factor correction characteristic.

Figure 3 shows the equivalent circuit of the proposed integrated electronic lighting driver circuit when the mode of operation is analyzed and illustrated. The following assumptions are made in analyzing the operating modes of the proposed integrated electronic lighting driver circuit.

- (a) The filter inductor L_f and the filter capacitor C_f are not considered when analyzing the operational modes of the proposed circuit.
- (b) The control of power switches S_1 and S_2 is a complementary signal, and their respective intrinsic diodes and parasitic capacitances, C_{S1} and C_{S2} , are considered.
- (c) Neglecting the conduction voltage drop and its equivalent resistance of all diodes.
- (d) The inductor L_B is designed to operate in discontinuous conduction mode (DCM).
- (e) The remaining circuit components are considered as ideal components.

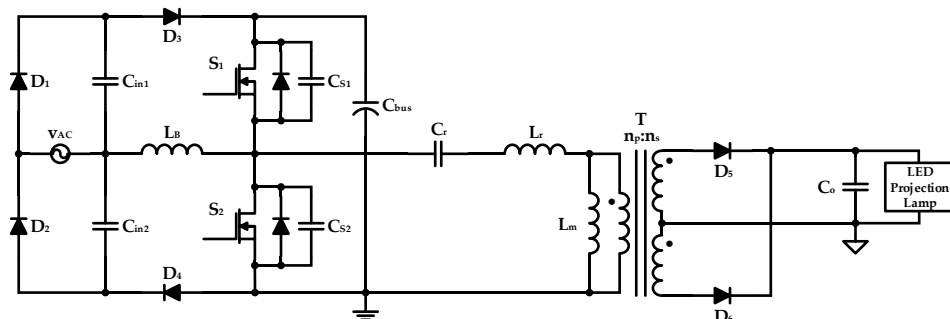


Figure 3. Equivalent circuit of the proposed integrated electronic lighting driver circuit while analyzing the operational modes.

The conduction and energy storage components of the input AC power v_{AC} are dominated by D_1, D_3 and C_{in1} in the positive half cycle, while the input AC power v_{AC} is dominated by D_2, D_4 and C_{in2} in the negative half cycle. The input AC power v_{AC} is first turned on by the power switch S_1 in the positive half cycle, and the input AC power v_{AC} is first turned on by the power switch S_2 in the negative half cycle. Figure 4 is the theoretical waveform of each important component when the input voltage is in the positive half cycle. The following action modes are analyzed and described when the input AC power v_{AC} is in the positive half cycle.

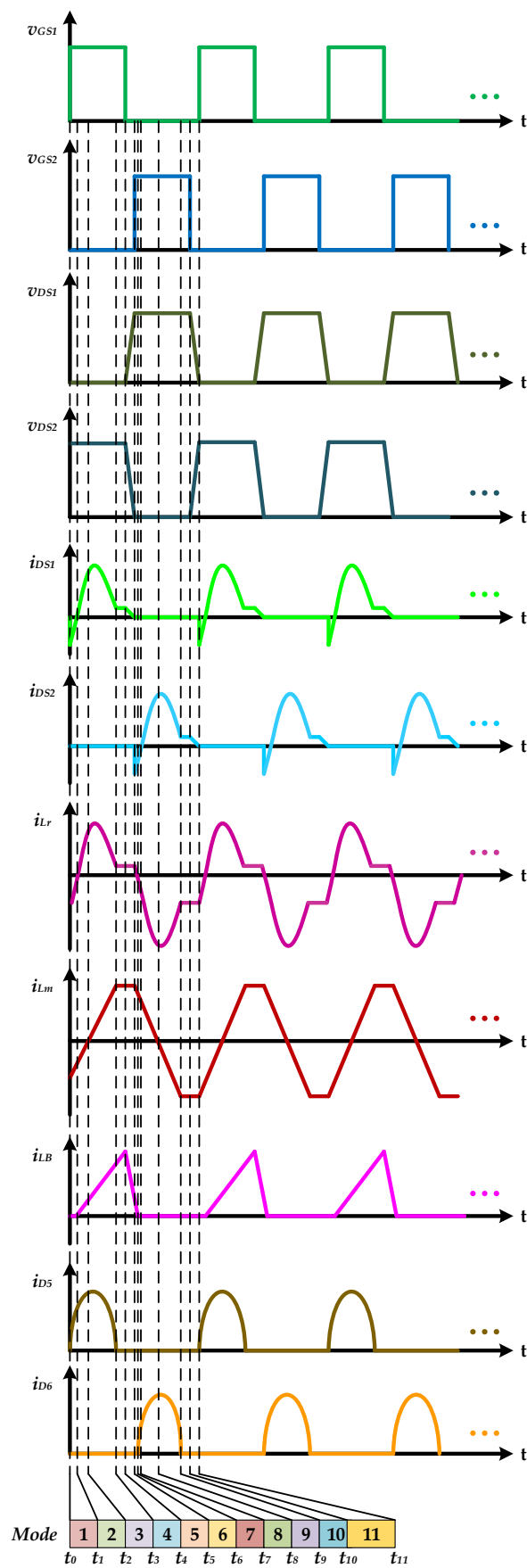


Figure 4. Theoretical waveforms of various important components when the input voltage is in the positive half cycle.

Operation Mode 1 ($t_0 \leq t < t_1$): Figure 5 shows the equivalent circuit of the proposed integrated electronic lighting driver for supplying an LED projection lamp during Mode 1. In the previous mode, the energy of the parasitic capacitor C_{S1} of the power switch S_1 is completely released, so the switch voltage v_{DS1} drops to zero, and the intrinsic diode of the switch S_1 is turned on at time t_0 . The input AC power v_{AC} provides energy to the input capacitor C_{in1} via the diode D_1 . The resonant inductance L_r and the magnetizing inductance L_m provide energy to the parasitic capacitor C_{S2} of the power switch S_2 , the DC link capacitor C_{bus} and the resonant capacitor C_r through the intrinsic diode of the switch S_1 and provide energy to the output capacitor C_o and the LED projection lamp through the transformer T and the output diode D_5 . In this mode, the magnetizing inductor current i_{Lm} decreases linearly. This mode ends when the current i_{DS1} of the power switch S_1 rises to zero.

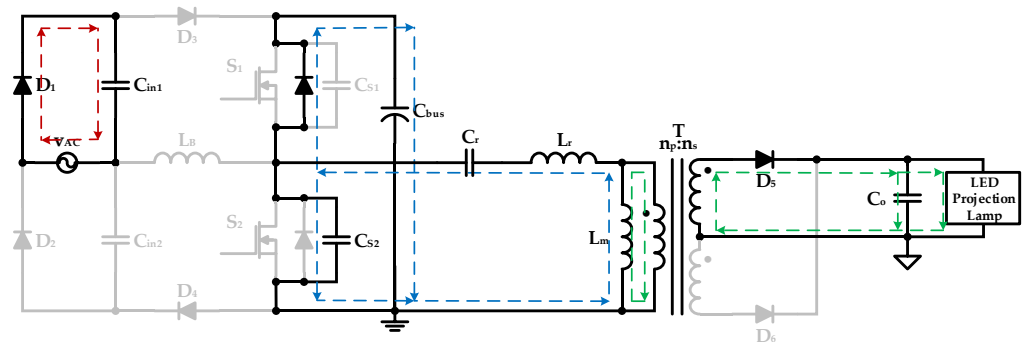


Figure 5. Equivalent circuit of the proposed integrated electronic lighting driver for supplying an LED projection lamp during Mode 1.

Operational Mode 2 ($t_1 \leq t < t_2$): Figure 6 shows the equivalent circuit of the proposed integrated electronic lighting driver for supplying an LED projection lamp during Mode 2. At time t_1 , the power switch S_1 is driven to conduct and achieves zero-voltage switching. The input AC power v_{AC} and the input capacitor C_{in1} provide energy to the boost inductor L_B through the diodes D_1 and D_3 and the switch S_1 , and the boost inductor current i_{LB} increases linearly. The DC link capacitor C_{bus} , the resonant capacitor C_r and the exciting inductor L_m provide energy to the resonant inductor L_r through the switch S_1 and provide energy to the output capacitor C_o and the LED projection lamp through the transformer T and the output diode D_5 . In this mode, the magnetizing inductor current i_{Lm} continues to display a linear decline. The DC link capacitor C_{bus} provides energy to the parasitic capacitor C_{S2} of the power switch S_2 via the switch S_1 . This mode ends when the magnetizing inductor current i_{Lm} reaches zero.

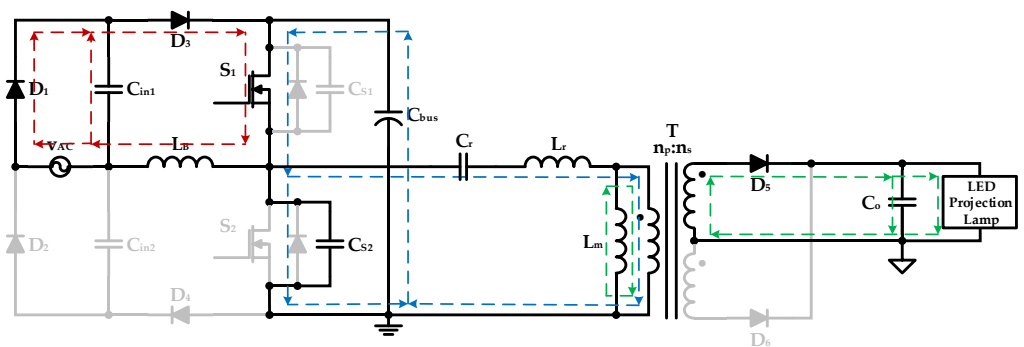


Figure 6. Equivalent circuit of the proposed integrated electronic lighting driver for supplying an LED projection lamp during Mode 2.

Operational Mode 3 ($t_2 \leq t < t_3$): Figure 7 shows the equivalent circuit of the proposed integrated electronic lighting driver for supplying an LED projection lamp during Mode 3.

The input AC power source v_{AC} and the input capacitor C_{in1} continuously provide energy to the boost inductor L_B through the diodes D_1 and D_3 and the switch S_1 , and the boost inductor current i_{LB} continues to display a linear increase. The DC link capacitor C_{bus} and the resonant capacitor C_r continuously provide energy to the resonant inductor L_r and the magnetizing inductor L_m through the switch S_1 and provide energy to the output capacitor C_o and the LED projection lamp through the transformer T and the output diode D_5 , and the magnetizing inductor current i_{Lm} linearly rises. The DC link capacitor C_{bus} continuously supplies energy to the parasitic capacitor C_{S2} of the power switch S_2 via the switch S_1 . This mode ends when the diode current i_{D5} drops to zero.

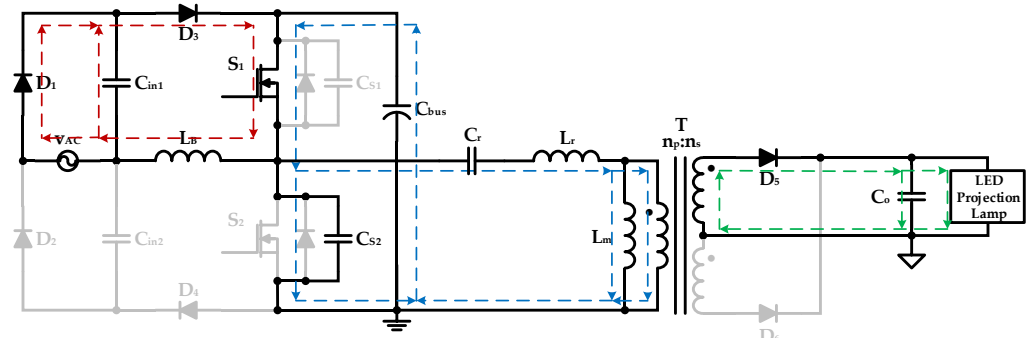


Figure 7. Equivalent circuit of the proposed integrated electronic lighting driver for supplying an LED projection lamp during Mode 3.

Operational Mode 4 ($t_3 \leq t < t_4$): Figure 8 shows the equivalent circuit of the proposed integrated electronic lighting driver for supplying an LED projection lamp during Mode 4. The input AC power source v_{AC} and the input capacitor C_{in1} continuously provide energy to the boost inductor L_B through the diodes D_1 and D_3 and the switch S_1 , and the boost inductor current i_{LB} continues to display a linear increase. The DC link capacitor C_{bus} and the resonant capacitor C_r continuously provide energy to the resonant inductor L_r and the magnetizing inductor L_m through the switch S_1 . The DC link capacitor C_{bus} continuously provides energy from the switch S_1 to the parasitic capacitor C_{S2} of the power switch S_2 . Since the inductor currents i_{Lr} and i_{Lm} in this mode are the same, no energy is transferred to the secondary side, and the energy of the LED projection lamp is provided by the output capacitor C_o . This mode ends when switch S_1 is turned off at time t_4 .

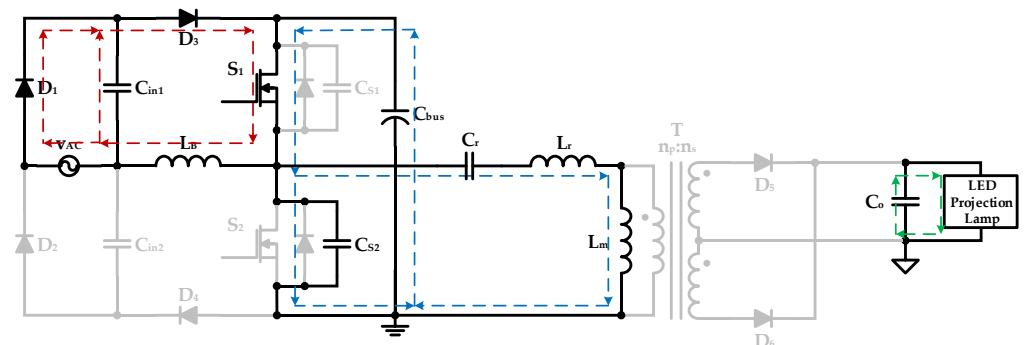


Figure 8. Equivalent circuit of the proposed integrated electronic lighting driver for supplying an LED projection lamp during Mode 4.

Operational Mode 5 ($t_4 \leq t < t_5$): Figure 9 shows the equivalent circuit of the proposed integrated electronic lighting driver for supplying an LED projection lamp during Mode 5. When the switch S_1 is turned off, the input AC power v_{AC} , the input capacitor C_{in1} and the boost inductor L_B provide energy to the parasitic capacitor C_{S1} and the DC link capacitor C_{bus} of the power switch S_1 through the diodes D_1 and D_3 , and the boost inductor current i_{LB} linearly declines. The DC link capacitor C_{bus} and the parasitic capacitor C_{S2} of

the power switch S_2 provide energy to the parasitic capacitor C_{S1} of the power switch S_1 , the resonant capacitor C_r , the resonant inductor L_r and the magnetizing inductor L_m . The output capacitor C_o continuously provides energy to the LED projection lamp. This mode ends when the switching voltage v_{DS2} drops to zero at time t_5 .

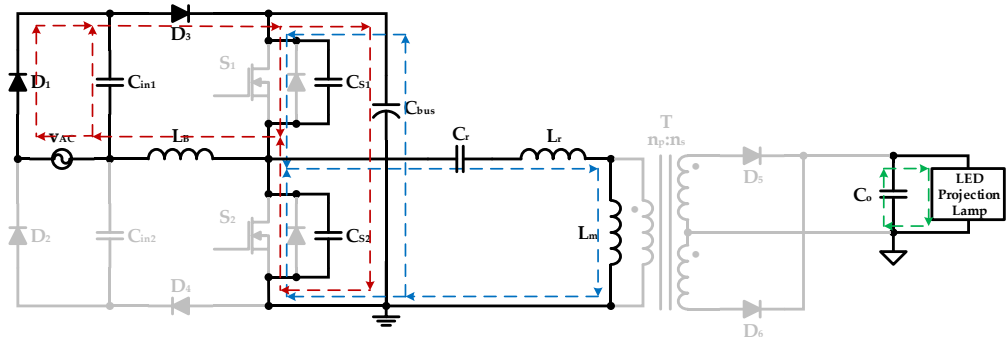


Figure 9. Equivalent circuit of the proposed integrated electronic lighting driver for supplying an LED projection lamp during Mode 5.

Operational Mode 6 ($t_5 \leq t < t_6$): Figure 10 shows the equivalent circuit of the proposed integrated electronic lighting driver for supplying an LED projection lamp during Mode 6. In the former mode, the energy stored in the parasitic capacitance C_{S2} of the switch S_2 is fully discharged, so the switching voltage v_{DS2} drops to zero, causing the intrinsic diode of the switch S_2 to conduct. The input AC power v_{AC} , the input capacitor C_{in1} and the boost inductor L_B provide energy to the DC link capacitor C_{bus} through the diodes D_1 and D_3 and the intrinsic diode of the switch S_2 , and the boost inductor current i_{LB} continues to decrease linearly. The DC link capacitor C_{bus} , the resonant inductor L_r and the magnetizing inductor L_m continue to provide energy to the resonant capacitor C_r and the parasitic capacitor C_{S1} of the power switch S_1 via the intrinsic diode of the switch S_2 , and the magnetizing inductor current i_{Lm} decreases linearly. The output capacitor C_o continuously provides energy to the LED projector lamp. This mode ends when the boost inductor current i_{LB} falls to zero.

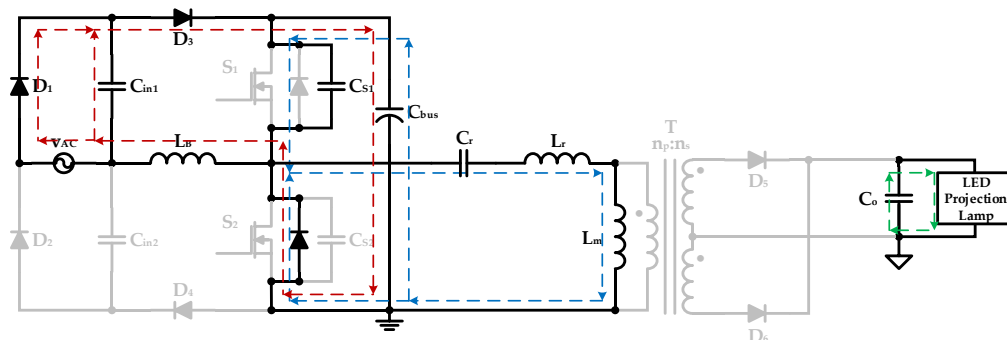


Figure 10. Equivalent circuit of the proposed integrated electronic lighting driver for supplying an LED projection lamp during Mode 6.

Operational Mode 7 ($t_6 \leq t < t_7$): Figure 11 shows the equivalent circuit of the proposed integrated electronic lighting driver for supplying an LED projection lamp during Mode 7. The input AC power v_{AC} provides energy to the input capacitor C_{in1} via the diode D_1 . The DC link capacitor C_{bus} , the resonant inductor L_r and the magnetizing inductor L_m continuously provide energy to the resonant capacitor C_r and the parasitic capacitor C_{S1} of the power switch S_1 through the intrinsic diode of the switch S_2 . In this mode, the magnetizing inductor current i_{Lm} presents a linear decline. The output capacitor C_o continuously provides energy to the LED projector lamp. This mode ends when the current i_{DS2} of the power switch S_2 rises to zero.

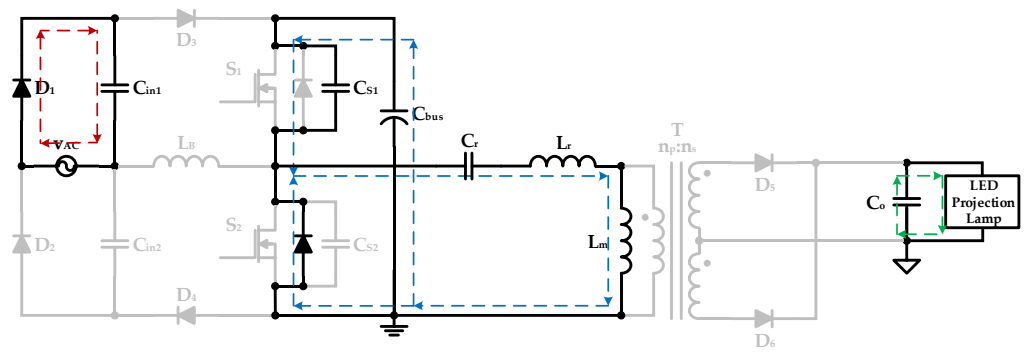


Figure 11. Equivalent circuit of the proposed integrated electronic lighting driver for supplying an LED projection lamp during Mode 7.

Operational Mode 8 ($t_7 \leq t < t_8$): Figure 12 shows the equivalent circuit of the proposed integrated electronic lighting driver for supplying an LED projection lamp during Mode 8. The power switch S_2 is driven to conduct and has the characteristic of zero voltage switching. The DC link capacitor C_{bus} provides energy to the parasitic capacitor C_{S1} of the switch S_1 via the power switch S_2 . The resonant capacitor C_r and the exciting inductor L_m provide energy to the resonant inductor L_r , the output capacitor C_o and the LED projection lamp via the switch S_2 , the transformer T and the diode D_6 . In this mode, the magnetizing inductor current i_{Lm} continues to show a linear decline. This mode ends when the magnetizing inductor current i_{Lm} drops to zero at time t_8 .

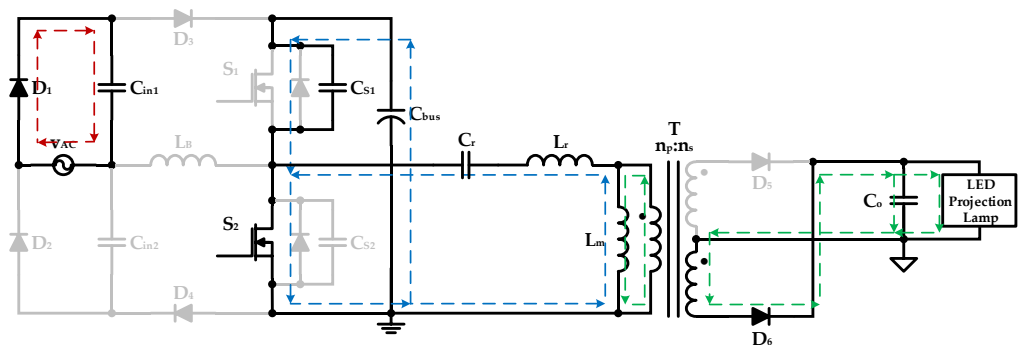


Figure 12. Equivalent circuit of the proposed integrated electronic lighting driver for supplying an LED projection lamp during Mode 8.

Operational Mode 9 ($t_8 \leq t < t_9$): Figure 13 shows the equivalent circuit of the proposed integrated electronic lighting driver for supplying an LED projection lamp during Mode 9. The DC link capacitor C_{bus} continuously provides energy to the parasitic capacitor C_{S1} of the switch S_1 via the power switch S_2 . The resonant capacitor C_r provides energy to the resonant inductor L_r , the magnetizing inductor L_m , the output capacitor C_o and the LED projection lamp via the switch S_2 , the transformer T and the diode D_6 . In this mode, the magnetizing inductor current i_{Lm} presents a linear rise. This mode ends when the diode current i_{D6} drops to zero.

Operational Mode 10 ($t_9 \leq t < t_{10}$): Figure 14 shows the equivalent circuit of the proposed integrated electronic lighting driver for supplying an LED projection lamp during Mode 10. The DC link capacitor C_{bus} continuously provides energy to the parasitic capacitor C_{S1} of the switch S_1 via the power switch S_2 . The resonant capacitor C_r continuously provides energy to the resonant inductor L_r and the magnetizing inductor L_m via the switch S_2 . Since the inductor currents i_{Lr} and i_{Lm} in this mode are the same, no energy is transferred to the secondary side, and the energy of the LED projection lamp is provided by the output capacitor C_o . This mode ends when switch S_2 is turned off at time t_{10} .

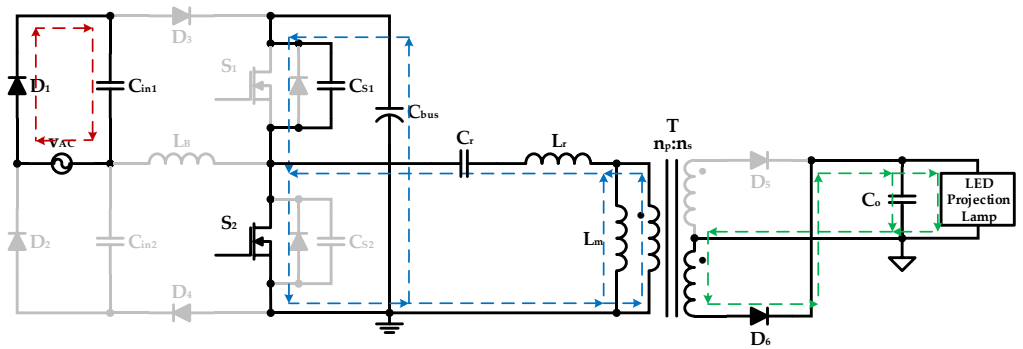


Figure 13. Equivalent circuit of the proposed integrated electronic lighting driver for supplying an LED projection lamp during Mode 9.

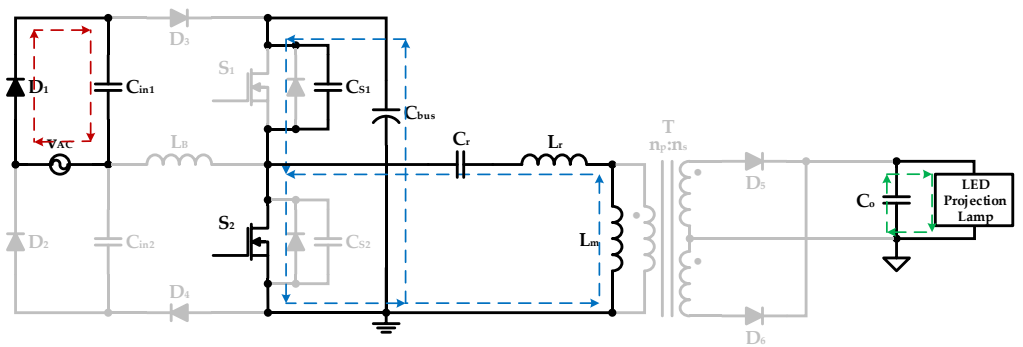


Figure 14. Equivalent circuit of the proposed integrated electronic lighting driver for supplying an LED projection lamp during Mode 10.

Operational Mode 11 ($t_{10} \leq t < t_{11}$): Figure 15 shows the equivalent circuit of the proposed integrated electronic lighting driver for supplying an LED projection lamp during Mode 11. When the switch S_2 is turned off, the parasitic capacitor C_{S1} and the resonant capacitor C_r of the power switch S_1 provide energy to the resonant inductor L_r , the magnetizing inductor L_m and the DC link capacitor C_{bus} . The output capacitor C_o continuously provides energy to the LED projector lamp. This mode ends when the voltage v_{DS1} of the parasitic capacitance C_{S1} of the switch S_1 drops to zero at time t_{11} . Afterwards, the circuit returns to the operation mode one.

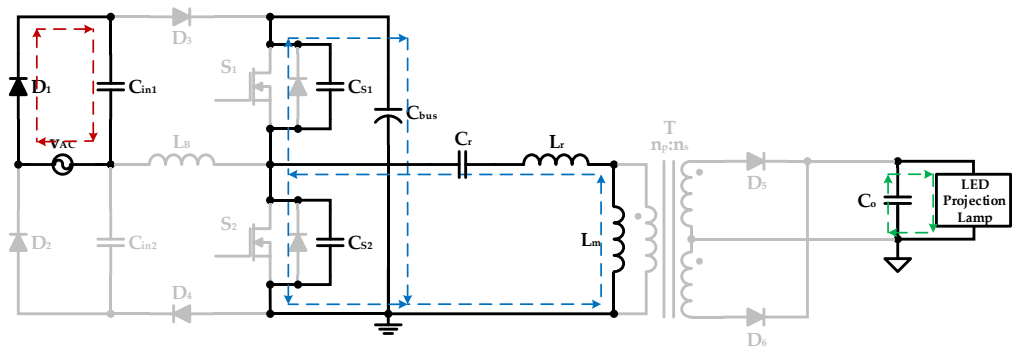


Figure 15. Equivalent circuit of the proposed integrated electronic lighting driver for supplying an LED projection lamp during Mode 11.

2.1. Design Guideline of the Inductor L_B

The theoretical vwaveform of voltage v_{LB} and current i_{LB} in the inductor L_B is shown in Figure 16. The peak value of the inductor current $I_{LB-peak}$ can be given by

$$I_{LB-peak} = \frac{V_{REC}}{2L_B} \times \left(\frac{T_S}{2} \right) \tag{1}$$

where V_{REC} and T_S are the voltage across the capacitors C_{in1} and C_{in2} and the switching period of the power switches, respectively. The rms value of the input AC current i_{AC-rms} is expressed by

$$i_{AC-rms} = \frac{P_O}{\eta V_{AC-rms}} \tag{2}$$

where P_O , V_{AC-rms} and η are the output power, the root-mean-square (rms) value of the input AC voltage and the estimated circuit efficiency, respectively. In addition, the peak value of the inductor current $I_{LB-peak}$ is equal to $\sqrt{2}$ times the input AC current i_{AC-rms} . By merging (1) with (2), the design guideline of the inductor L_B can be expressed as

$$L_B = \frac{\eta V_{AC-rms} \times V_{REC}}{2\sqrt{2}P_O} \times \left(\frac{T_S}{2} \right) \tag{3}$$

With a V_{AC-rms} of 110 V, a P_O of 100 W, an η of 0.9 and a switching period T_S of 1/(100 kHz), the inductances of the inductor L_B are calculated as

$$L_B = \frac{0.9 \times 110 \times 156}{2\sqrt{2} \times 100} \times \left(\frac{1}{2 \times 100k} \right) = 273 \mu\text{H}$$

In order to provide the driver circuit with a power factor correction function, the inductor L_B is designed to operate in the discontinuous conduction mode, and the inductor L_B was selected to be 221 μH when the prototype driver circuit was realized.

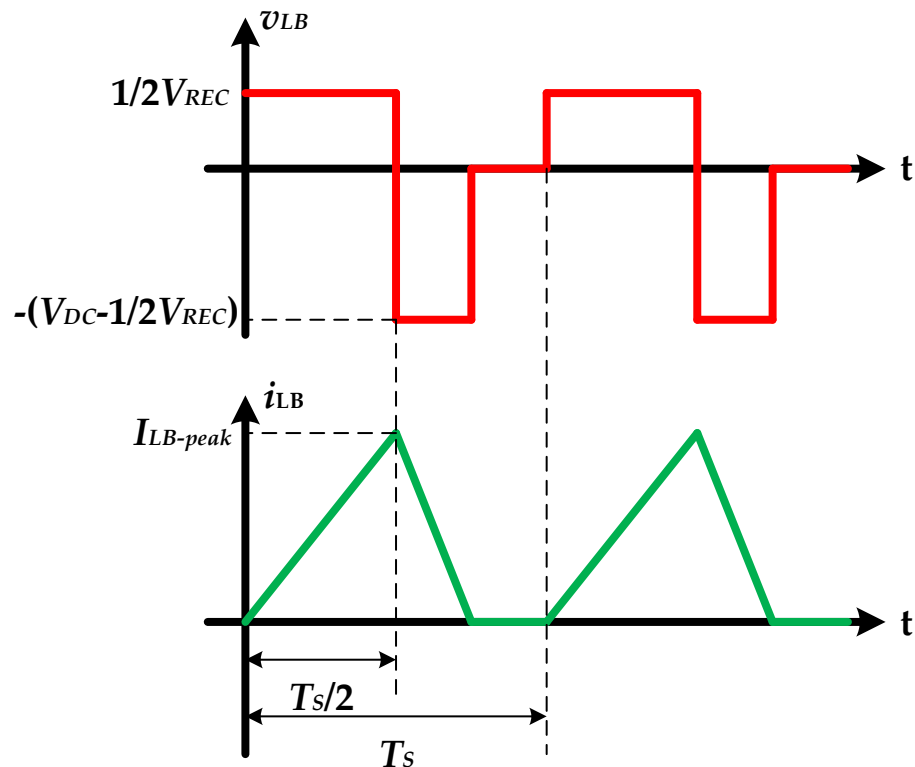


Figure 16. The theoretical waveform of the voltage v_{LB} and current i_{LB} in the inductor L_B .

2.2. Design Consideration of the Turns Ratio n in the Transformer T

The turns ratio n in the transformer T can be expressed by

$$n = \frac{n_p}{n_s} = \frac{V_{DC} \times Duty}{V_O + V_F} \quad (4)$$

where V_{DC} , $Duty$, V_O and V_F are the voltage across the capacitor C_{bus} , the duty cycle of the power switches, the output voltage and the voltage drop of the output diode, respectively. With a V_{DC} of 380 V, a $Duty$ of 0.45, a V_O of 36 V and a V_F of 1.3 V, the turns ratio n is calculated as

$$n = \frac{n_p}{n_s} = \frac{380 \times 0.45}{36 + 1.3} = 4.58$$

In addition, the turns ratio n is selected to be 4.7 when implementing the prototype driver circuit.

3. Experimental Results of the Proposed AC-DC Integrated Electronic Lighting Driver Circuit for Supplying an LED Projection Lamp

Figure 17 is a photograph of the LED projection lamp used in the experiments in this paper, which consists of two high-power LEDs rated at 50 watts each. The specifications of the LED projection lamp used in the experiment are as follows: the rated power is 100 W, the rated input voltage is 36 V, the rated input current is 2.77 A, the luminous efficiency is greater than 119 lm/W, the color rendering index is greater than 80 and the weight is 3.5 kg. The IP (International Protection) rating system was drafted by the IEC (International Electrotechnical Commission) and classifies electrical appliances according to their dust and moisture resistance. The IP protection rating consists of two numbers, the first number indicating the level of protection of the device against ingress of dust and foreign matter, and the second number indicating the level of protection of the device against ingress of moisture and water into the airtightness of the device. The level of protection means that external objects (including tools, human fingers, etc.) must not come into contact with the electrical parts of the appliance to avoid electric shock. In addition, the larger the number, the higher the level of protection. Moreover, the dustproof and waterproof grade of the experimental projection lamp is IP 66. The first number of the protection class 6 is a class with a dustproof effect, and it is defined as the complete prevention of the intrusion of foreign objects, although it cannot completely prevent the entry of dust, but the amount of dust that intrudes will not affect the normal operation of the appliance. The second number of protection level 6 is the level of protection against the intrusion of large waves, and it is defined as the protection of electrical appliances installed on the deck against damage caused by the intrusion of large waves. A prototype of the proposed electronic lighting driver circuit has been successfully developed and proved to supply an LED projection lamp with a power rating of 100 W, with an input mains line voltage of 110 V. Table 1 shows the circuit specifications of the proposed AC-DC integrated electronic lighting driver circuit for supplying an LED projection lamp, and the switching frequency is 100 kHz. Table 2 depicts the key components utilized in the proposed AC-DC integrated electronic lighting driver circuit. A high-voltage resonant controller (STMicroelectronics L6599AT) is used in the proposed electronic lighting driver circuit that powers the LED projector lamp and integrates all the necessary functions to properly control the two power switches in the half-bridge LLC resonant topology. In addition, the high-voltage resonant controller generates the two gate-driving signals for the two power switches by means of a control scheme with a fixed duty cycle of approximately 50% and a variable frequency of operation, and it can be used to regulate the output voltage and current of the LED projection lamp.



Figure 17. Photograph of the LED projection lamp used for the experiment in this paper.

Table 1. Specifications of the Proposed AC-DC Electronic Lighting Driver Circuit for Supplying an LED Projection lamp.

Parameter	Value
Input AC Voltage v_{AC}	110 V
Rated Output Power P_O	100 W
Rated Output Voltage V_O	36 V
Rated Output Current I_O	2.77 A
Switching Frequency	100 kHz

Table 2. Key Components Used in the Proposed AC-DC Electronic Lighting Driver Circuit for Supplying an LED Projection lamp.

Component	Value
Filter Inductor L_f	2.88 mH
Filter Capacitor C_f	100 nF
Diodes D_1, D_2, D_3, D_4	VS-3C06ET07T-M3
Capacitors C_{in1}, C_{in2}	1 μ F
Inductor L_B	220 μ H
Diodes D_5, D_6	VS-3C06ET07T-M3
Power Switches S_1, S_2	STP20NM60
DC-Linked Capacitor C_B	330 μ F/450 V
Resonant Inductor L_r	143 μ H
Resonant Capacitor C_r	15 nF
Magnetic Inductor L_m	740 μ H

The measured inductor current i_{LB} and its zoomed-in waveform are shown in Figure 18a,b, respectively. As shown in the measured waveforms, the inductor current i_{LB} is running in a DCM and therefore can reach the function of power factor correction. Figure 19 displays the measured waveforms of the switch voltage v_{DS1} and switch current i_{DS1} ; measurements show the presence of ZVS on switch S_1 , which reduces switching losses and improves circuit efficiency.

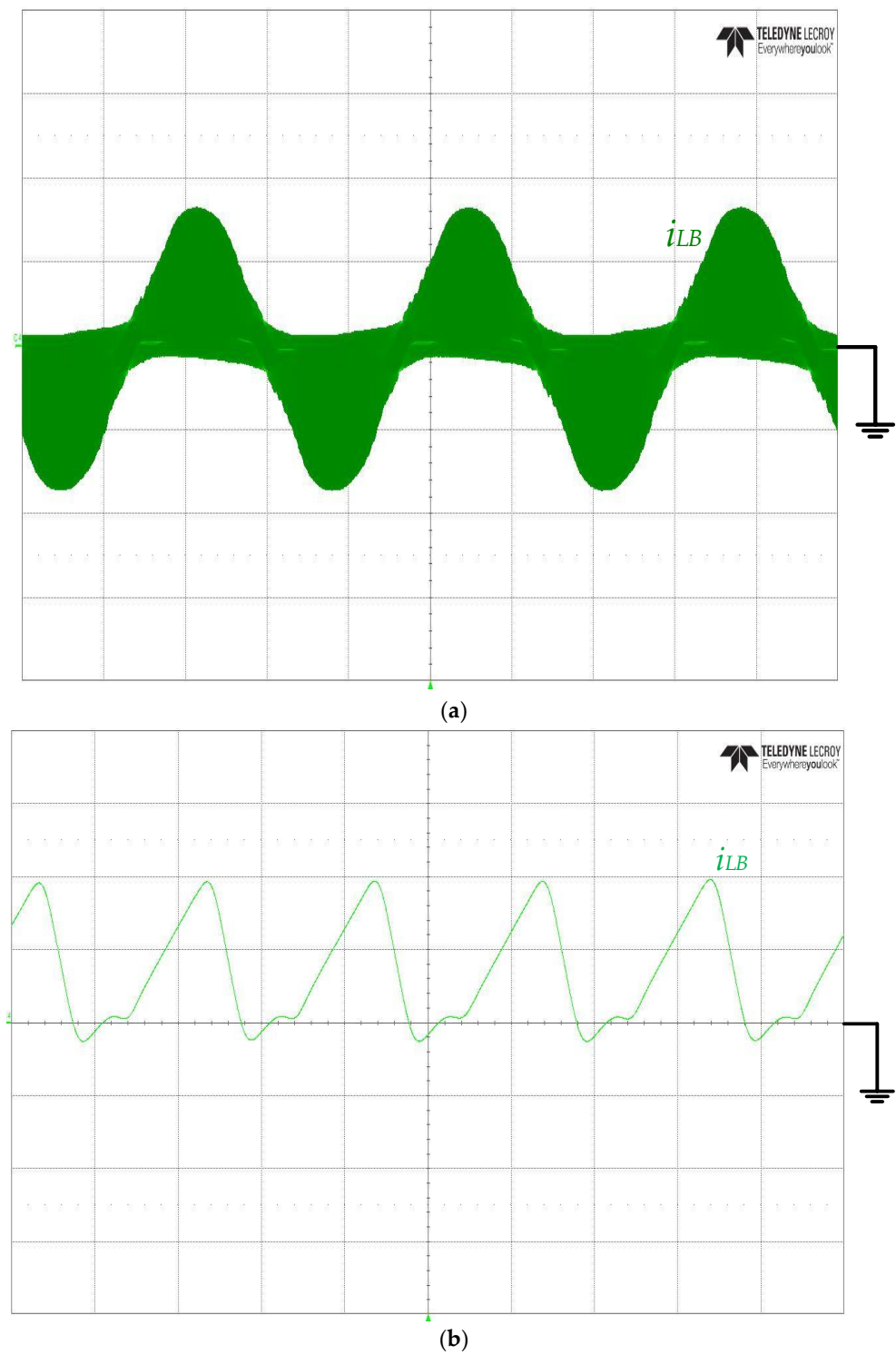


Figure 18. (a) Measured inductor current i_{LB} (2 A/div); time scale: 5 ms/div. (b) Zoomed-in inductor current i_{LB} (1 A/div); time scale: 5 μ s/div.

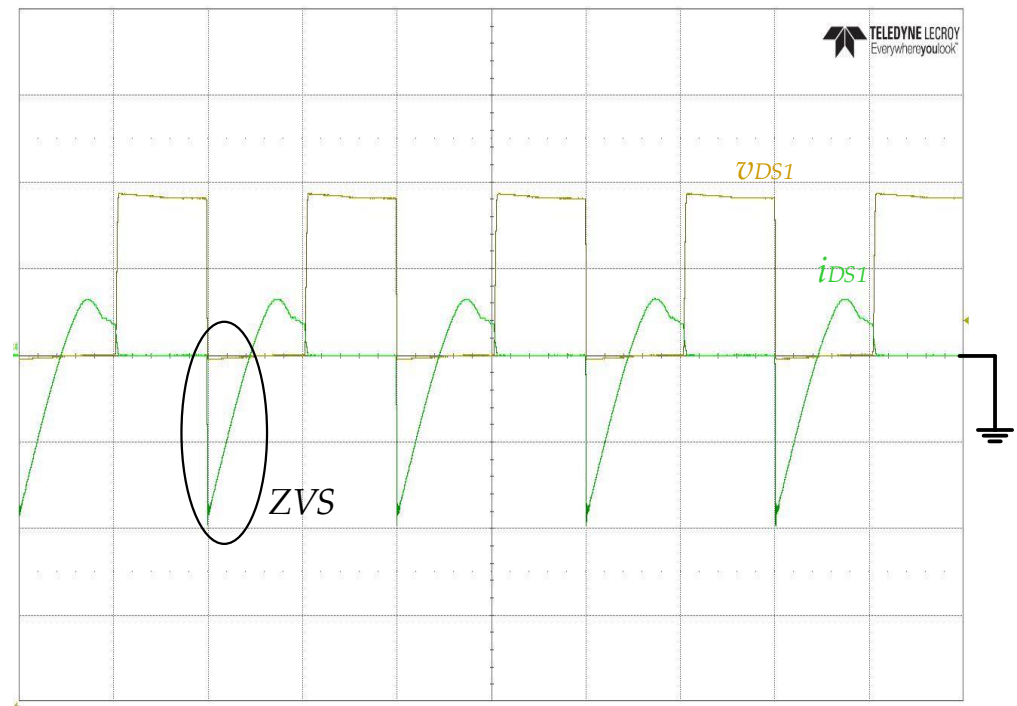


Figure 19. Measured waveforms of the switch voltage v_{DS1} (200 V/div) and the switch current i_{DS1} (2 A/div); time scale: 5 μ s/div.

Figure 20 displays the measured waveforms of the switch voltage v_{DS1} and the resonant inductor current i_{Lr} . Figure 21 shows the measured switch voltage v_{DS1} and diode current i_{D5} ; thus, it can be seen that ZCS occurs on the power diode. Figure 22 displays the measured waveforms of the output voltage V_o and output current I_o . The average values of the output voltage V_o and output current I_o are, respectively, about 36 V and 2.8 A. Figure 23 displays the measured waveforms of the output voltage ripple $V_{o,ripple}$ and the output current ripple $I_{o,ripple}$. Table 3 shows the measured output voltage ripple and current ripple of the presented electronic lighting driver circuit for an LED projection lamp. The mean value and peak-to-peak value of the output voltage are 35.818 V and 2.54 V, respectively. Additionally, the mean value and peak-to-peak value of the output current are 2.8574 A and 184.7 mA, respectively. The definition of the ripple factor of the output voltage and output current is derived by dividing the peak-to-peak value by the average value of the output voltage and output current. Moreover, the measured output voltage and output current ripple factors are 7.091% and 6.4639%, respectively.

Table 3. Measured ripple factors of the output voltage and output current in the presented integrated electronic lighting driver circuit for supplying an LED projection lamp.

Parameters	Values
Peak-to-peak value of the output voltage	2.54 V
Mean value of the output voltage	35.818 V
Ripple factor of the output voltage	7.091%
Peak-to-peak value of the output current	184.7 mA
Mean value of the output current	2.8574 A
Ripple factor of the output current	6.4639%

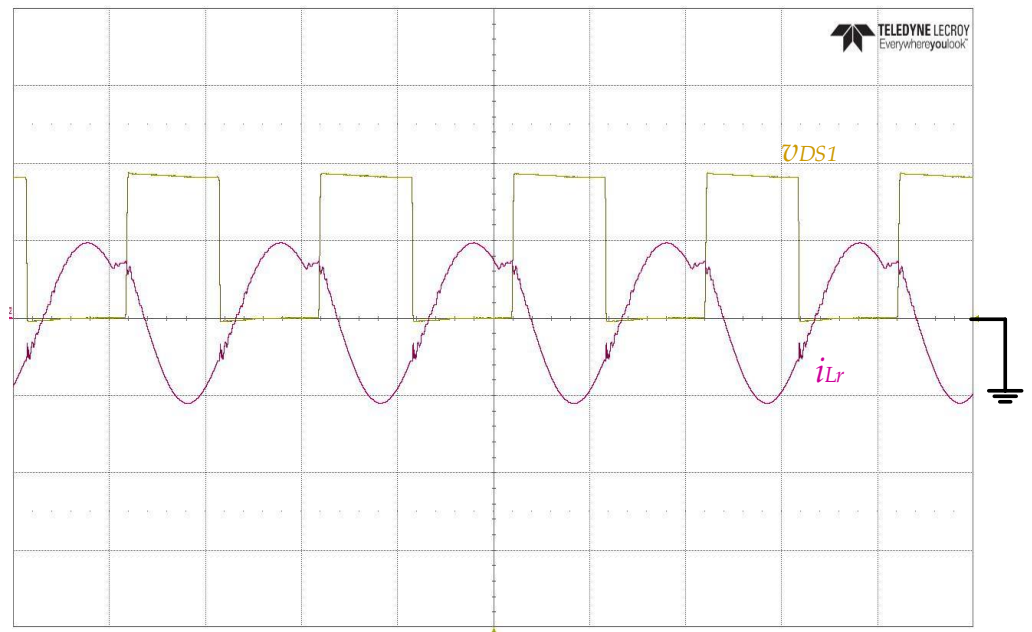


Figure 20. Measured waveforms of the switch voltage v_{DS1} (200 V/div) and the resonant inductor current i_{Lr} (1 A/div); time scale: 5 μ s/div.

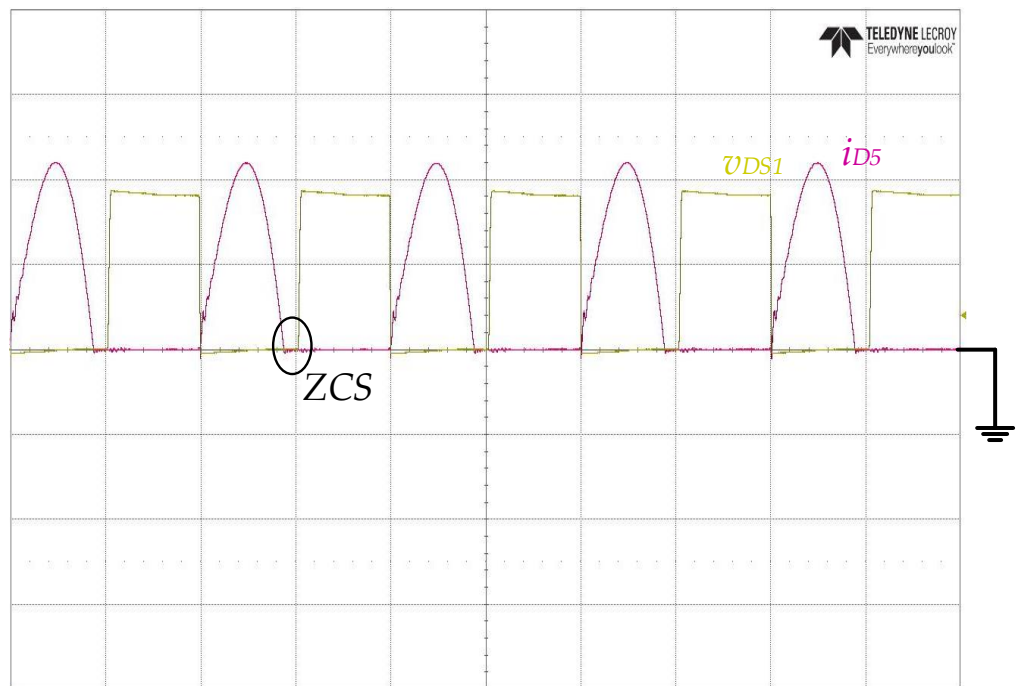


Figure 21. Measured waveforms of the switch voltage V_{DS1} (200 V/div) and the diode current i_{D5} (2 A/div); time scale: 5 μ s/div.

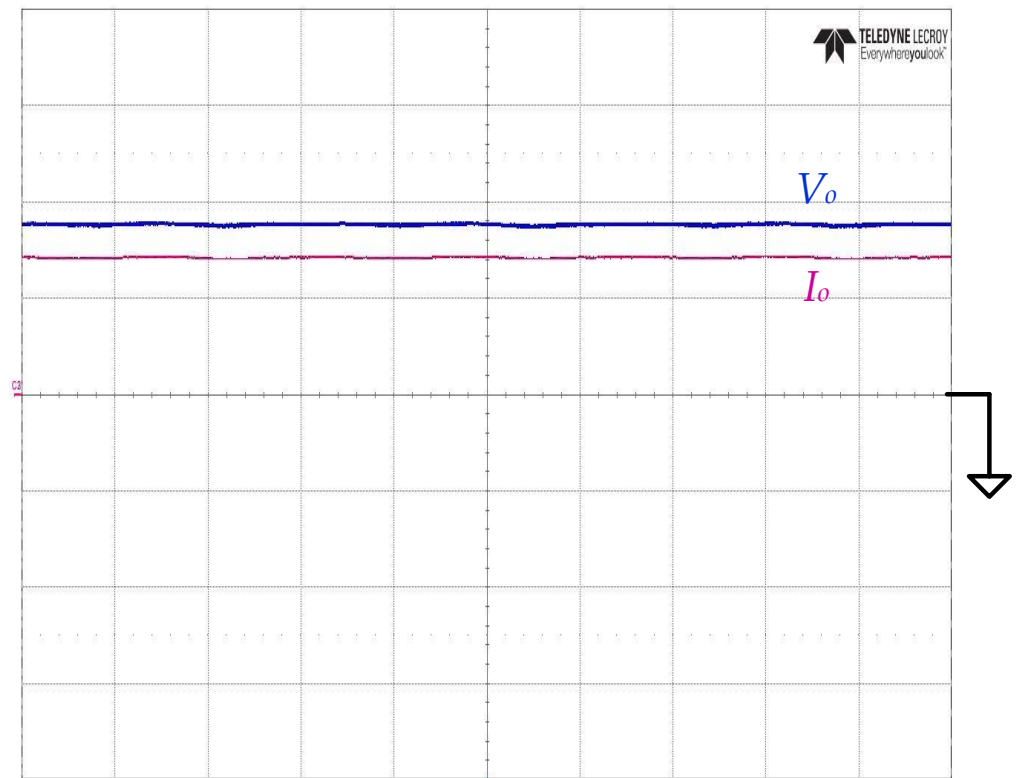


Figure 22. Measured waveforms of the output voltage V_o (20 V/div) and the output current I_o (2 A/div); time scale: 5 ms/div.

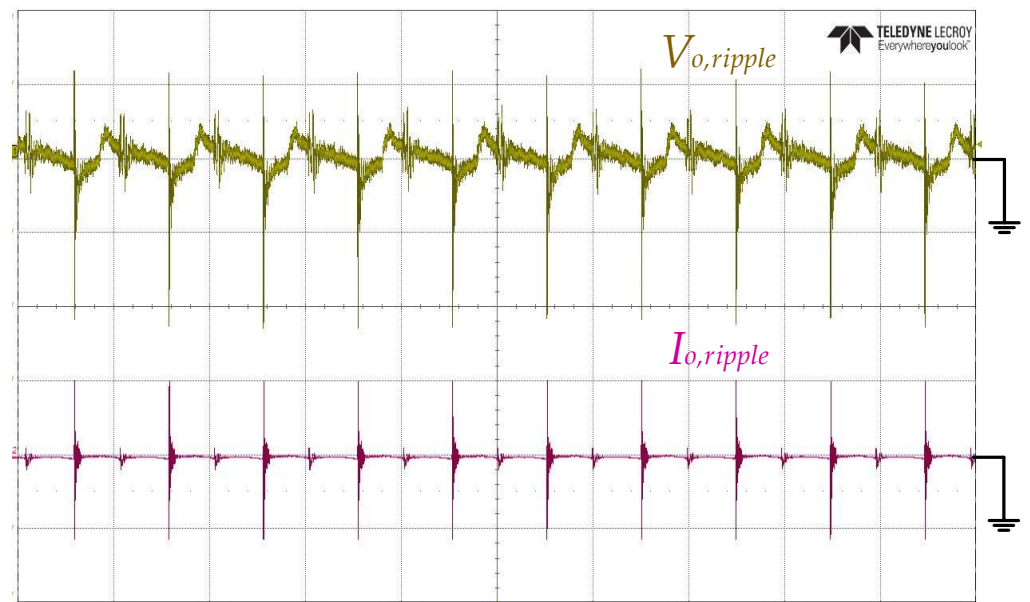


Figure 23. Measured waveforms of the output voltage ripple $V_{o,ripple}$ (1 V/div) and the output current ripple $I_{o,ripple}$ (200 mdiv); time scale: 10 μ s/div.

The measured waveforms of the input voltage v_{in} and input current i_{in} are shown in Figure 24. The input current i_{in} follows the input utility-line voltage v_{in} , which shows that the electronic lighting driver circuit developed in this paper has the function of power factor correction. Figure 25 shows the measured values of the input currents of the prototype LED projector lamp driver circuit for each order of harmonics and the standard values specified in IEC 61000-3-2 Class C [28] using a power analyzer with a 110-volt AC input

voltage. As can be seen in Figure 25, the measured input current harmonic values of all orders are lower than the standard values stipulated in IEC 61000-3-2 Class C.

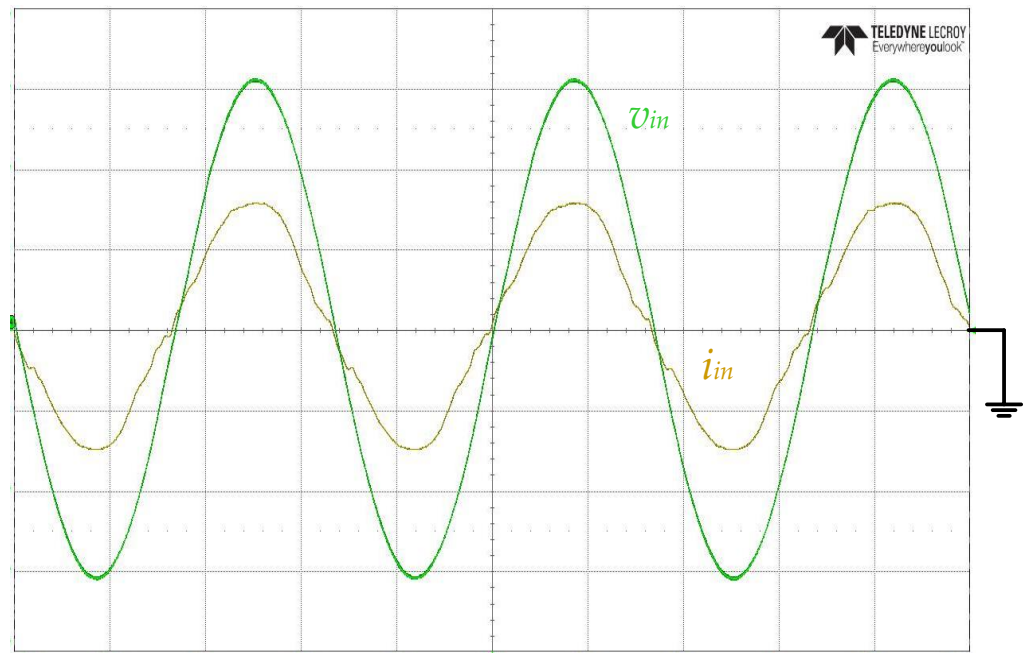


Figure 24. Measured input utility-line voltage v_{in} (50 V/div) and current i_{in} (1 A/div); time scale: 5 ms/div.

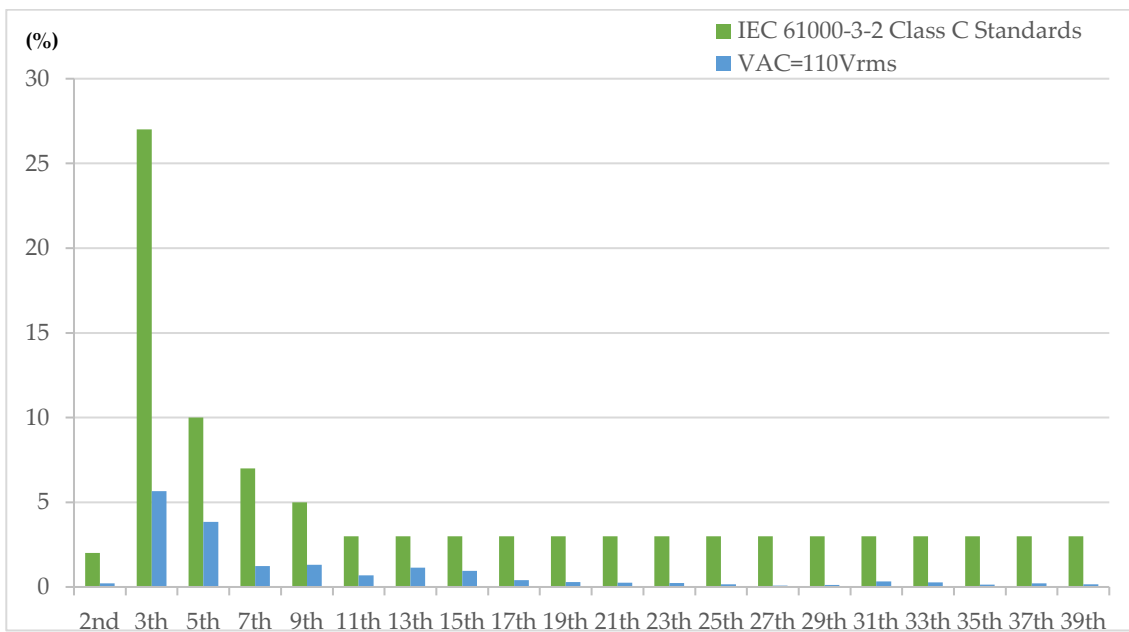


Figure 25. Measured input utility line current harmonics compared to the IEC 61000-3-2 Class C standard.

By using a power analyzer, the measured results of the power factor and total harmonic distortion of the input current in the proposed integrated electronic lighting driver circuit for providing an LED projection lamp with an input utility-line voltage of 110 V are 0.9879 and 5.7951%, respectively. Moreover, the measured circuit efficiency of the propsoed driver circuit is 89.85%. Figure 26 displays a photograph of the single-stage integrated electronic lighting driver circuit for supplying the experimental LED projection lamp.

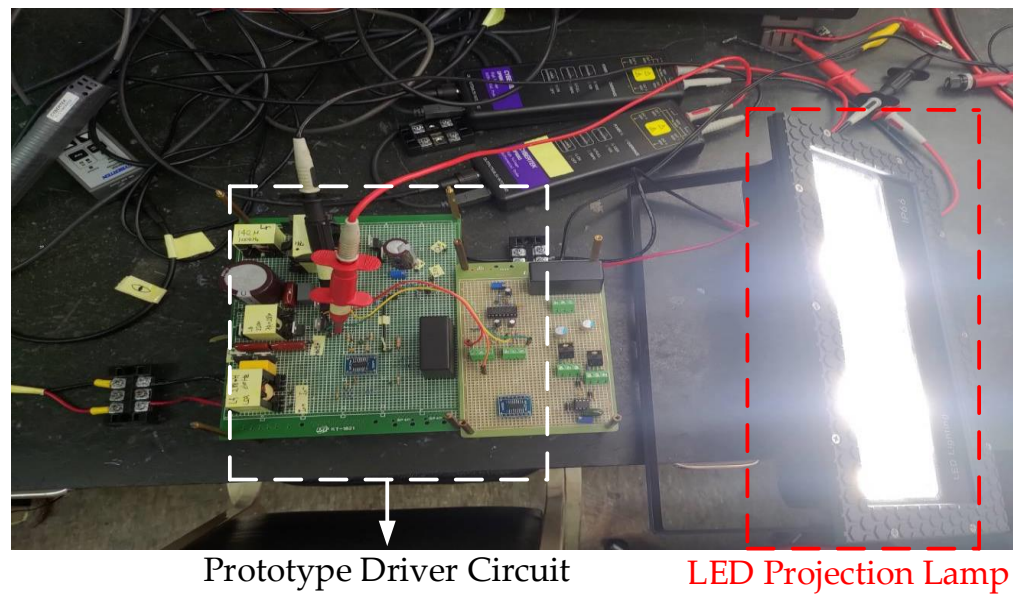


Figure 26. Photograph of the proposed integrated electronic lighting driver circuit for supplying with the LED projection lamp.

Moreover, Figure 27 shows the loss breakdown chart of the proposed integrated electronic lighting driver circuit for supplying with the LED projection lamp. In addition, the conduction loss of a power switch can be calculated by multiplying the square of the switch current by the equivalent resistance of the power switch used, while the conduction loss of a power diode can be calculated by multiplying the diode current by the forward voltage drop of the power diode. As shown in Figure 27, it can be revealed that the percentages of conduction losses of the power diode (D_1, D_2), the power diode (D_3, D_4), the power diode (D_5, D_6), the power switch (S_1, S_2) and other losses are 13.60%, 14.48%, 17.93%, 3.65% and 50.34%, respectively.

Table 4 shows comparisons between the existing two-stage and single-stage AC-DC driver circuit suitable for powering the LED projection lamp in [18,29,30] and the proposed one. As can be seen from Table 4, the proposed LED driver circuit saves a power switch and a diode compared to the existing two-stage one. In addition, the proposed LED driver circuit saves one magnetic element and four diodes compared to the existing single-stage LED driver circuit in [29] and six diodes compared to the existing single-stage LED driver circuit in [30].

Table 4. Comparisons between the existing two-stage and single-stage AC-DC driver circuit suitable for powering the LED projection lamp in [18,29,30] and the proposed one.

Item	Existing Two-Stage AC-DC LED Driver Circuit in Reference [18]	Existing Single-Stage AC-DC LED Driver Circuit in Reference [29]	Existing Single-Stage AC-DC LED Driver Circuit in Reference [30]	Proposed AC-DC LED Driver Circuit
Circuit Topology	Quasi-Resonant Dual Buck Converter and LLC Resonant Converter	Integration of an interleaved buck-boost converter with coupled inductors and an LLC resonant converter	Integration of an interleaved buck converter with a coupled inductor and an HB-SR converter with an FB rectifier	Integration of a modified stacked boost converter and a half-bridge LLC resonant converter

Table 4. Cont.

Item	Existing Two-Stage AC-DC LED Driver Circuit in Reference [18]	Existing Single-Stage AC-DC LED Driver Circuit in Reference [29]	Existing Single-Stage AC-DC LED Driver Circuit in Reference [30]	Proposed AC-DC LED Driver Circuit
Number of Required Switches	3	2	2	2
Number of Required Capacitors	6	6	6	6
Number of Required Magnetic Elements	4	5	4	4
Number of Required Diodes	7	10	12	6

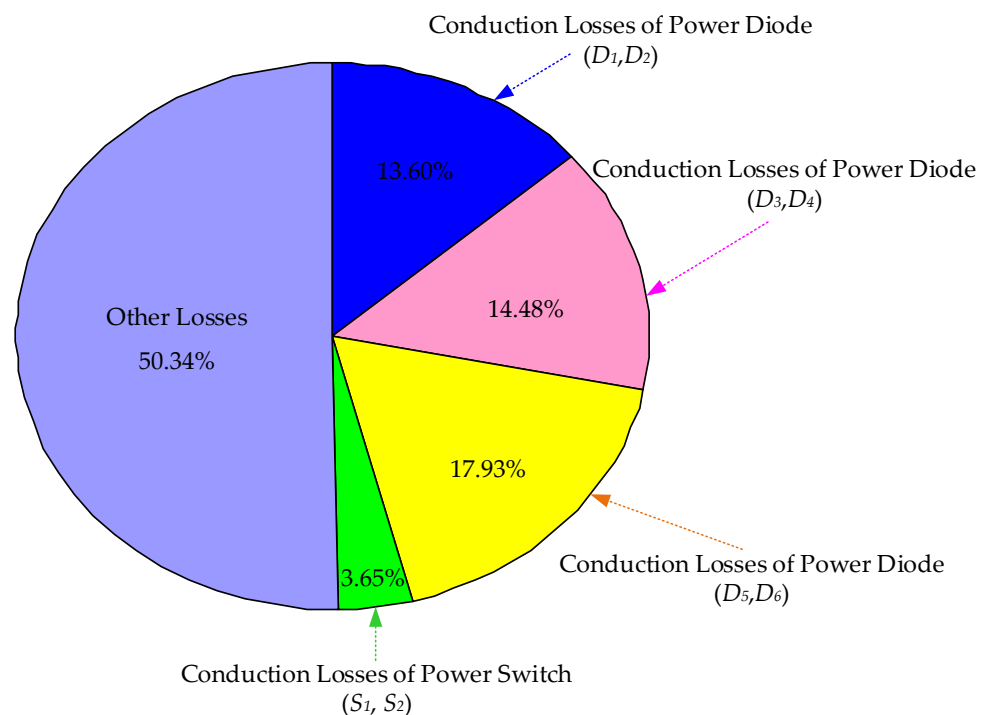


Figure 27. The loss breakdown chart of the proposed integrated electronic lighting driver circuit for supplying with the LED projection lamp.

4. Conclusions

This paper presents a new LED projection lamp electronic lighting driver circuit that integrates a modified stacked dual boost converter with factor correction and a half-bridge LLC resonant converter into a single-stage circuit architecture. By operating the inductor design of the modified stacked dual boost converter in discontinuous conduction mode, the power factor correction can be achieved naturally. The new LED projection lamp electronic lighting driver circuit realizes zero-voltage switching of the power switch and zero-current switching of the output diode, which reduces the loss of power components and improves the circuit efficiency. In addition, the number of components used in the driver circuit is less than in previous two-stage and single-stage circuit topologies. In this paper, a 100 W prototype driver circuit for LED projector light electronic lighting has been developed and tested. At an AC input voltage of 110 volts RMS and at a rated output power, the results of the prototype driver circuit were: an output voltage ripple rate less than 8%, an output current ripple rate less than 7%, a power factor greater than 0.98, an input current total harmonic distortion factor less than 6% and a circuit efficiency greater

than 89%, thus verifying the functionality of the presented driver circuit for powering the LED projection lamp.

Author Contributions: C.-A.C. developed and designed the circuit topology; C.-M.L. and E.-C.C. arranged and performed circuit simulations; S.-H.H., L.-F.L. and C.-K.L. carried out the prototype driver circuit and measured as well as analyzed the experimental results with guidance from C.-A.C.; C.-A.C. revised the manuscript for submission. All authors have read and agreed to the published version of the manuscript.

Funding: This research was funded by the National Science and Technology Council (NSTC) of Taiwan for its grants (grant numbers MOST 111-2221-E-214-011 and NSTC 112-2221-E-214-005).

Data Availability Statement: The data presented in this study are available in this article.

Conflicts of Interest: The authors declare no conflict of interest.

References

1. Website of OSRAM for Projection Applications. Available online: <https://www.osram.com/pia/applications/projection/index.jsp?mkt=/projection/> (accessed on 20 September 2023).
2. Website of Projection Lamps Information. Available online: https://www.globalspec.com/learnmore/optics_optical_components/light_sources/projection_lamps (accessed on 20 September 2023).
3. Website of PHILIPS for LED Outdoor Lighting Products. Available online: <https://www.lighting.philips.com/prof/outdoor-luminaires> (accessed on 20 September 2023).
4. Website of GE Lighting for LED Flood Lights & Spotlights. Available online: <https://www.gelighting.com/led-lights/bulb-types/spot-flood-lights> (accessed on 20 September 2023).
5. Branás, C.; Azcondo, F.J.; Alonso, J.M. Solid-State Lighting: A System Review. *IEEE Ind. Electron. Mag.* **2013**, *7*, 6–14. [CrossRef]
6. VBender, V.C.; Marchesan, T.B.; Alonso, J.M. Solid-State Lighting: A Concise Review of the State of the Art on LED and OLED Modeling. *IEEE Ind. Electron. Mag.* **2015**, *9*, 6–16. [CrossRef]
7. Fang, P.; Liu, Y.-F.; Sen, P.C. A Flicker-Free Single-Stage Offline LED Driver With High Power Factor. *IEEE J. Emerg. Sel. Top. Power Electron.* **2015**, *3*, 654–665. [CrossRef]
8. Khalilian, H.; Farzanehfard, H.; Adib, E.; Esteki, M. Analysis of a New Single-Stage Soft-Switching Power-Factor-Correction LED Driver With Low DC-Bus Voltage. *IEEE Trans. Ind. Electron.* **2018**, *65*, 3858–3865. [CrossRef]
9. Menke, M.F.; Seidel, A.R.; Tambara, R.V. LLC LED Driver Small-Signal Modeling and Digital Control Design for Active Ripple Compensation. *IEEE Trans. Ind. Electron.* **2019**, *66*, 387–396. [CrossRef]
10. Gagliardi, G.; Lupia, M.; Cario, G.; Tedesco, F.; Cicchello Gaccio, F.; Lo Scudo, F.; Casavola, A. Advanced Adaptive Street Lighting Systems for Smart Cities. *Smart Cities* **2020**, *3*, 1495–1512. [CrossRef]
11. Sędziwy, A.; Kotulski, L. Towards Highly Energy-Efficient Roadway Lighting. *Energies* **2016**, *9*, 263. [CrossRef]
12. Garcia-Caparros, P.; Chica, R.M.; Almansa, E.M.; Rull, A.; Rivas, L.A.; García-Buendía, A.; Barbero, F.J.; Lao, M.T. Comparisons of Different Lighting Systems for Horticultural Seedling Production Aimed at Energy Saving. *Sustainability* **2018**, *10*, 3351. [CrossRef]
13. Gago-Calderón, A.; Hermoso-Orzáez, M.J.; De Andres-Diaz, J.R.; Redrado-Salvatierra, G. Evaluation of Uniformity and Glare Improvement with Low Energy Efficiency Losses in Street Lighting LED Luminaires Using Laser-Sintered Polyamide-Based Diffuse Covers. *Energies* **2018**, *11*, 816. [CrossRef]
14. Luo, Q.; Huang, J.; He, Q.; Ma, K.; Zhou, L. Analysis and Design of a Single-Stage Isolated AC–DC LED Driver With a Voltage Doubler Rectifier. *IEEE Trans. Ind. Electron.* **2017**, *64*, 5807–5817. [CrossRef]
15. Spini, C. *AN3106-48V-130W High-Efficiency Converter with PFC for LED Street Lighting Applications*; STMicroelectronics Application Note; STMicroelectronics: Geneva, Switzerland, 2016; pp. 1–31.
16. Narahariseti, K.; Green, P.B. *Design of 200 W Boost PFC Plus HB LLC Resonant Converter with IR1155, IRS27952 and IR11688*; Infineon Technologies, Application Note AN_1907_PL88_1908_004522; Infineon Technologies: Hong Kong, China, 2020; pp. 1–98.
17. YWang, Y.; Guan, Y.; Xu, D.; Wang, W. A CLCL Resonant DC/DC Converter for Two-Stage LED Driver System. *IEEE Trans. Ind. Electron.* **2016**, *63*, 2883–2891. [CrossRef]
18. Wang, Y.; Gao, S.; Zhang, S.; Xu, D. A Two-Stage Quasi-Resonant Dual-Buck LED Driver With Digital Control Method. *IEEE Trans. Ind. Appl.* **2018**, *54*, 787–795. [CrossRef]
19. Arias, M.; Lamar, D.G.; Linera, F.F.; Balocco, D.; Diallo, A.A.; Sebastián, J. Design of a Soft-Switching Asymmetrical Half-Bridge Converter as Second Stage of an LED Driver for Street Lighting Application. *IEEE Trans. Power Electron.* **2012**, *27*, 1608–1621. [CrossRef]
20. Wang, Y.; Guan, Y.; Zhang, X.; Xu, D. Single-stage LED driver with low bus voltage. *Electron. Lett.* **2013**, *49*, 455–457. [CrossRef]
21. Wang, Y.; Guan, Y.; Huang, J.; Wang, W.; Xu, D. A Single-Stage LED Driver Based on Interleaved Buck–Boost Circuit and LLC Resonant Converter. *IEEE J. Emerg. Sel. Top. Power Electron.* **2015**, *3*, 732–741. [CrossRef]
22. Wang, Y.; Qi, N.; Guan, Y.; Cecati, C.; Xu, D. A Single-Stage LED Driver Based on SEPIC and LLC Circuits. *IEEE Trans. Ind. Electron.* **2017**, *64*, 5766–5776. [CrossRef]

23. Wang, Y.; Hu, X.; Guan, Y.; Xu, D. A Single-Stage LED Driver Based on Half-Bridge CLCL Resonant Converter and Buck–Boost Circuit. *IEEE J. Emerg. Sel. Top. Power Electron.* **2019**, *7*, 196–208. [CrossRef]
24. Cheng, C.-A.; Chang, E.-C.; Lee, C.-M.; Lan, L.-F.; Hou, S.-H.; Lin, C.-K. A novel driver circuit for supplying LED projection lamps with high-power-factor and soft-switching. In Proceedings of the 25th International Conference on Mechatronics Technology (ICMT 2022), Kaohsiung City, Taiwan, 18–21 November 2022; pp. 1–4.
25. Cheng, C.A.; Cheng, H.L.; Chang, C.H.; Chang, E.C.; Lan, L.F.; Hsu, H.F. A novel driver circuit for piezoelectric ceramic actuator featuring with input-current-shaping and soft-switching. In Proceedings of the 25th International Conference on Mechatronics Technology (ICMT 2022), Kaohsiung City, Taiwan, 18–21 November 2022; pp. 1–4.
26. “Effective Use of Power Devices- Silicon Carbide Power Devices Understanding & Application Examples Utilizing the Merits”, ROHM Semiconductor. 2017. Available online: https://pages.rohm.com.tw/rs/247-PYD-578/images/TechWeb_E_DL_SiC.pdf (accessed on 7 November 2023).
27. “SiC Power Devices and Modules Application Note”, ROHM Semiconductor. 2020. Available online: https://fscdn.rohm.com/en/products/databook/applinote/discrete/sic/common/sic_appli-e.pdf (accessed on 20 September 2023).
28. IEC 61000-3-2; Wikipedia, the Free Encyclopedia. Available online: https://en.wikipedia.org/wiki/IEC_61000-3-2 (accessed on 20 September 2023).
29. Cheng, C.A.; Chang, C.H.; Cheng, H.L.; Chang, E.C.; Chung, T.Y.; Chang, M.T. A Single-Stage LED Streetlight Driver with Soft-Switching and Interleaved PFC Features. *Electronics* **2019**, *8*, 911. [CrossRef]
30. Cheng, C.A.; Cheng, H.L.; Chang, C.H.; Chang, E.C.; Kuo, Z.Y.; Lin, C.K.; Hou, S.H. An AC-DC LED Integrated Streetlight Driver with Power Factor Correction and Soft-Switching Functions. *Sustainability* **2023**, *15*, 10579. [CrossRef]

Disclaimer/Publisher’s Note: The statements, opinions and data contained in all publications are solely those of the individual author(s) and contributor(s) and not of MDPI and/or the editor(s). MDPI and/or the editor(s) disclaim responsibility for any injury to people or property resulting from any ideas, methods, instructions or products referred to in the content.